INTERNATIONAL SOCIETY FOR SOIL MECHANICS AND GEOTECHNICAL ENGINEERING

SIMSG | ISSMGE

Surface ground motion measurements to assess complexity in site response

M. Pontrelli & L.G. Baise
Tufts University, Medford, MA, USA

ABSTRACT: Strong impedance contrasts are known to play a role in soil amplification both from the fundamental physics of conservation of energy across a strong impedance contrast and from observations with examples from around the world. From prior work by the author and others (Thompson et al., 2009; Thompson et al., 2012), we know that a strong peak in the weak motion surface/borehole transfer function is consistent with resonance due to vertical propagation of shear waves through horizontally layered soil systems. The shape of the transfer function can be altered by scattering through heterogeneous materials, significant attenuation, non-vertical incidence, and other complexities in the subsurface. In this work, we focus on evaluating site response complexity using only surface stations. Microtremor studies using Nakamura's technique (Nakamura, 1989), which is the ratio of the Fourier amplitude noise spectra of the horizontal component to that of the vertical component (H/V), have proven useful in strong impedance-contrast environments to estimate the fundamental site period, sediment thickness, and ultimately soil amplification. H/V ratios have also been used to evaluate site response using earthquake ground motions. While fundamental site period is reliably estimated with H/V ratios, the amplification is sensitive to the noise environment and the signal processing and therefore, is not generally trusted. In this work, we focus on the shape of the peak in H/V ratios as an indicator of site response complexity. Using earthquake recordings from Mexico City, we demonstrate that H/V ratios can be used as an indicator of complexity in site response, in a similar manner to that demonstrated by Thompson et al. (2012) using surface/borehole transfer functions. In Mexico City, non-resonant H/V ratios are consistent with the transition zone at the edge of the Lake Bed sediments.

1 INTRODUCTION

Recent work in earthquake site response (Thompson et al., 2009; Rathje et al., 2010; Rodriguez-Marek et al., 2011; Thompson et al., 2012; Kaklamanos et al., 2013; Kaklamanos et al., 2015; Zalachoris and Rathje, 2015; Griffiths et al., 2016; Teague and Cox, 2016; Cabas et al., 2017; Teague et al., 2018) has focused on the challenges of accurately predicting earthquake site response. The assumption of one-dimensional propagation of shear waves (SH1D) using equivalent linear and nonlinear soil models often does not provide sufficient prediction accuracy. The challenges in predicting site response include: input motion variability (Rathje et al., 2010); heterogeneity of soil properties (Thompson et al., 2009; 2012); uncertainty in the Vs profile (Griffiths et al., 2016; Teague and Cox, 2016; Teague et al., 2018); three-dimensional structure (Baise et al., 2003; Thompson et al., 2012); and uncertainty in the characterization of damping and kappa (Zalachoris and Rathje, 2015; Cabas et al., 2017). Thompson et al. (2012) proposed a taxonomy on site response complexity that used weak ground motions from vertical array sites to determine if common wave propagation assumptions were valid. The taxonomy uses two key criteria: 1) inter-event variability of the transfer function and 2) the similarity between the empirical and one-dimensional theoretical transfer function. In this work, we extend this taxonomy for use with single surface stations by utilizing the H/V ratio.

1.1 Site response

Given an earthquake at a large hypocentral distance from two stations with the same recording instrument, a and b, we assume that the source, path and instrument response of these stations are equal, thus the transfer function, $a(f)$, from station b to station a is represented by the ratio of the amplitude response spectra of station a and station b.

$$a(f) = \frac{S_a(f)}{S_b(f)} \tag{1}$$

Traditional site response studies have used two methods to estimate the site response $a(f)$: standard spectral ratio using a reference site, and surface-downhole spectral ratio (Borcherdt, 1970; Campillo et al. 1985, Shearer and Orcutt, 1987; Lermo and Chávez-Garcia 1994; Thompson et al. 2012; Kaklamanos, 2015; Kaklamanos, 2018). These methods, however, have limitations: standard spectral ratios require a reference site that meets certain criteria (Steidl, 1996) and boreholes are expensive and intrusive in already developed areas. Due to these limitations, researchers have explored the potential of Nakamura's H/V ratio (Nakamura, 1989) as a first estimate of site response (Lermo and Chávez-Garcia, 1994; Parolai, 2002). The H/V ratio method is non-intrusive, requires one three component seismometer station and can use microtremor data, thus allowing for rapid, cheap field collection (Yilar et al. 2017). We use the H/V ratio as a first estimate of $a(f)$ to map site complexity using earthquake ground motion records from seismic stations in the RACM network in Mexico City.

1.2 Geology of Mexico City

Mexico City was built at the location of three historic shallow lakes: Texcoco, where most of the urban sprawl is now located, Xochimilco, to the southwest of Texcoco and south of Cerro de la Estrella and Chalco, to the southeast of Texcoco and west-southwest of Cerro del la Estrella. The three lakes were filled with windblown volcanic ash during the Wisconsin glacial period and are now characterized by compressible, high plasticity, high water content clays interspersed with horizontal lenses of sand and soil layers (Romo, 1988). The lakes were shallow and therefore never formed any significant deltas while the ash was settling, leaving the lake sediments mostly laterally homogenous (Stephenson and Lomnitz, 2004). The general stratigraphy of the lakes is a 1-2 meter crust underlain by 25-30 meters Upper Clay Formation (UCF) underlain by the roughly 3 meter thick First Hard Layer (FHL) underlain by around 20 meters of Lower Clay Formation (LCF) until the Deep Deposits (DD) (Figure 1b) (Romo, 1988; Stephenson and Lomnitz, 2004). For engineering purposes, this stratigraphy represents the half space we use for our theoretical transfer function calculation with the DD as the high velocity basement (Romo 1988). The UCF has a V_s around 70 m/s, the FHL has a shear wave velocity around 200 m/s, the LCF has a shear wave velocity around 100 m/s and the deep deposits have a shear wave velocity of around 475 m/s, calculated from an SCPT and SASW test (Stephenson and Lomnitz, 2004; Mayoral et al. 2016). This is the typical profile for the lake beds: a high impedance contrast, due to the low density, low shear wave velocity UCF and LCF lake sediments overlying the high shear wave velocity high density deep deposits, and a laterally homogenous soft soil layer, a geologic structure indicative of soil amplification that can be modeled with a one-dimensional theoretical transfer function.

The Transition zone of Mexico City is defined as the edge of the old lakes where the depth to the deep deposits is less than 20 meters (Moises et al. 2016). This stratigraphy is like that of the lake zone but with shallower depth and more significant lenses of sand within the clay layer due to stream runoff into the lake (Moises et al. 2016). Characterized by shallower depths to the deep deposits, greater heterogeneity than the lake zone, and a dipping halfspace, we expect higher fundamental frequencies and greater transfer function complexity in the transition zone than the lake zone.

2 DATA

Following the 1985 Michoacán earthquake, the RACM network was installed in Mexico City to provide ground motion data for basic research to assess and mitigate vulnerability within the Valley of Mexico. Since 1987, 78 devices have recorded 224 events at 72 surface and 8 borehole stations (CIRES website). We computed H/V ratios at 68 stations within the clay-lake area and transition zone using all events available at each station to estimate the site H/V ratio and its inter-event variability. This station list excludes the 8 borehole stations, and 2 stations classified in the hill zone. We removed recordings which had significant instrument or digitizing error, plotting waveforms with nearly flat magnitude responses. After cleaning, the stations have an average of 78, minimum of 21 and maximum of 183 events per station. In this paper, we present the results at eight stations for illustration.

3 METHODS

3.1 *Empirical transfer function*

We compute the empirical transfer function $a(f)$ (equation 1) from the Mexico City RACM ground motion data using Nakamura's H/V ratio, which is the amplitude spectra of the horizontal component divided by the amplitude spectra of the vertical component. We use the entire ground motion of each event provided in the database which contaminates the frequency content of the S-wave with the entire ground motion but simplifies processing. We prefer this strategy as we include many recordings in our analysis. We apply a two-pole low-pass Butterworth filter (Butterworth, 1930) with a high corner frequency of 49 Hz, one Hz below the Nyquist frequency of the stations with lowest sampling frequency, in the forward and reverse direction to all three components of every record at the 68 stations in the transition and lake zone. We then combine the horizontal time records using the two-dimensional (2D) complex time-series of the two horizontal time series from Steidl et al. (Steidl, 1994) and compute the magnitude spectra of the combined and filtered recording using the absolute value of the FFT function in MATLAB. Finally, we smooth the magnitude spectra using a triangular moving average filter with width 0.1 Hz. Next, we compute the H/V ratio by dividing the combined horizontal amplitude spectra by the vertical. We do this for every event recorded at the station and combine the H/V ratios using the median of $a(f)$, which is given by the maximum likelihood estimator:

$$\hat{a}(f) = exp\left(\frac{1}{n}\sum_{i=1}^{n}\ln[a_i(f)]\right) \tag{2}$$

where $a_i(f)$ is the $a(f)$ for i = 1,...,n ground motions. We plot $\hat{a}(f)$ with a large sample $100(1-\alpha)$ confidence interval given as:

$$exp\left(\ln[\hat{a}(f)] \pm z_{1-\alpha/2} \times \sigma_{ln}(f)\right) \tag{3}$$

with standard deviation:

$$\sigma_{ln}(f) = \sqrt{\frac{1}{n}\sum_{i=1}^{n}\left(\ln[a_i(f)] - \ln[\hat{a}(f)]\right)^2} \tag{4}$$

We generate figures with frequencies between 0 and 5 Hz because we found that beyond 5 Hz, the H/V ratios tend to approach unity and the predominant fundamental building frequencies lie in this range. The $\hat{a}(f)$ for site CE32 in the lake zone is also shown in Figure 2.

3.2 *Theoretical transfer function*

The theoretical transfer function (TTF) estimates a site transfer function given a horizontally layered soil profile with inputs: soil layer thickness (h_i), shear wave velocity (V_{si}) density (ρ_i) and intrinsic attenuation ($^iQ_s^{-1}$) where i is the soil layer number overlying a high velocity basement with shear wave velocity (V_b) and density (ρ_i). (Thomson, 1950; Haskell, 1953; 1960). We use the Thomson-Haskell TTF, computed using the Fortran program Nrattle from Boore (2005) ground motion simulation program SMSIM. The TTF assumes (1) the medium is laterally homogenous; (2) wavefronts are planar; (3) only the SH wave is modelled and (4) damping is frequency independent. These assumptions are collectively referred to as the SH1D response model (Thompson et al. 2012).

To look at how the shape of the peak of the H/V ratio compares to the shape of the TTF, we fit the TTF to $\hat{a}(f)$ (equation 2) using a simple one clay layer stratigraphy over the deep deposit half space, omitting, for now, the FHL and LCL. We select V_s and ρ values for the clay layer of 73 m/s, and 1.1 g/cm^3 respectively and V_s and ρ values for the deep deposits of 475 m/s and 2.7 g/cm^3 respectively, parameters derived from SASW and SCPT shear wave velocity and geologic profiles from Romo, 1988; Stephenson et al. 2004; and Mayoral et al. 2016. We do not use V_s average from the DD to the surface for the approximated single clay layer because we must assume either depth or shear wave velocity. In order to compute V_s average from the shear wave velocity profile computed in Stephenson et al. 2004 or Mayoral et al. 2016, we need to know the depth to the DD. Our inversion *solves* for depth using an estimated V_s from the literature assuming that the clay layer is a single layer of entirely homogenous material. A solution to this problem would be to use the GIS contour map of the DD depths derived from geotechnical borehole data published by Moisés et al. 2016. Knowing the depths at each station would allow us to compute a V_s average using one of the available shear wave velocity profiles. We then search for the values of $^iQ_s^{-1}$ and h by minimizing the sum of squared residuals between the first and fourth peaks of the TTF and $\hat{a}(f)$ (equation 2) for stations in the lake zone and minimizing the sum of squared residuals of the entire TTF and $\hat{a}(f)$ for stations in the transition zone using the differential evolutionary algorithm from scipy.optimize. We need to use different objective functions for the lake zone and the transition zone because we observed several distinct peaks in the lake zone $\hat{a}(f)$ (Figure 2) that can be fit using the taxonomy of Thompson et al. 2012 (section 3.3) and only one broad peak in the $\hat{a}(f)$ at stations in the transition zone (Figure 3) that can't be fit using the first to fourth peaks of the TTF. The TTF for site CE32 in the lake zone is shown in Figure 1a.
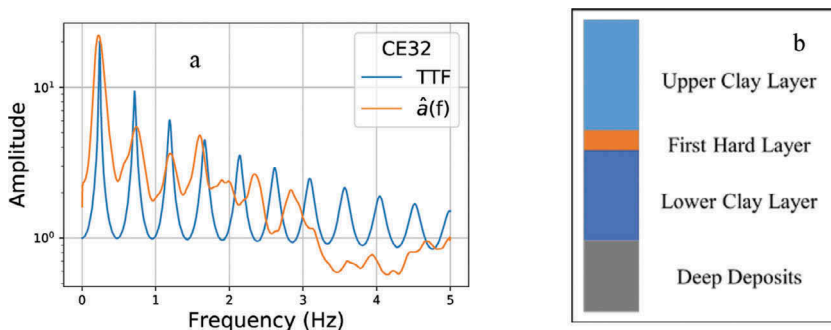

Figure 1. (a) TTF-$\hat{a}(f)$ matching, the TTF is in blue and $\hat{a}(f)$ is in orange computed from a ground motion record at station CE32. The TTF values are: V_s and ρ of first layer = 73 m/s and 1.1 g/cm^3 respectively, V_s and ρ of second layer = 475 m/s and 2.7 g/cm^3 respectively, h = 76.77 m and $^iQ_s^{-1}$ = 0.05. (b) Generalized soil profile for the lake area.

3.3 *Taxonomy from* Thompson et al. 2012

To classify the sites into SH1D or complex, we use the taxonomy described in Thompson et al. 2012. This taxonomy uses two criteria to classify stations: the interevent variability and the goodness of fit to the SH1D transfer function. The interevent variability is defined as the median σ_{ln} (equation 4) of the ETF between the first and fourth peaks of the SH1D transfer function denoted as σ_i. A station with $\sigma_i > 0.35$ is considered to have high interevent variability and a station with $\sigma_i < 0.35$ is considered to have low interevent variability.

The second criteria for defining site complexity from Thompson et al. 2012 is goodness of fit to the SH1D transfer function, defined by the Pearson correlation coefficient r of the TTF and $\hat{a}(f)$ (equation 2) between the first and fourth peaks of the TTF. A site is considered a good fit to the SH1D transfer function if it has an r value greater than 0.6 and a poor fit if it has an r value less than 0.6. Given both criteria, there are four classifications for site complexity: LG, LP, HP and HG where the first letter denotes either "low" or "high" σ_i and the second letter denotes either "good" or "poor" fit to the SH1D transfer function. A site classified as LG has a good fit to the SH1D and can be used to calibrate and validate one-dimensional constitutive models. After computing $\hat{a}(f)$ with 95% confidence interval (equation 3) at all the stations in the study, we selected four H/V ratios at stations in the lake zone (Figure 2) and four H/V ratios at stations in the transition zone (Figure 3) to evaluate.
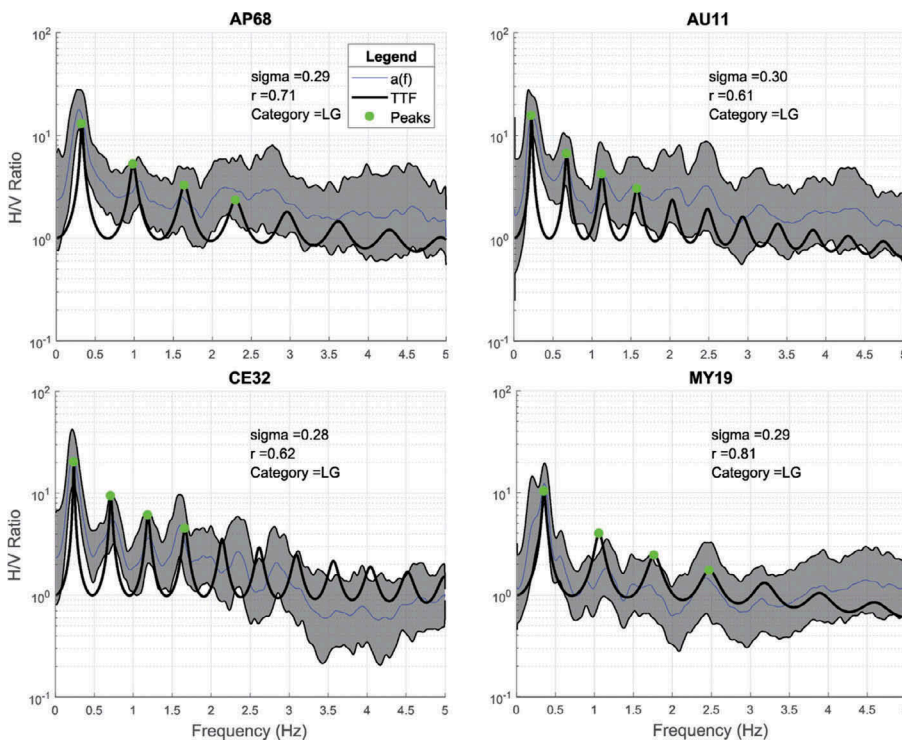

Figure 2. H/V ratios from the lakebed zone. The σ_i values for stations AP68, AU11, CE32 and MY19 are 0.29, 0.30, 0.28 and 0.29 respectively and their r values are 0.71, 0.61, 0.62, and 0.81 respectively. Thus, they are all classified as low inter-event variability and good fit to the SH1D transfer function. The green dots show the four peaks of the theoretical transfer function between which the σ_i and r statistic were computed.

4 RESULTS

4.1 *H/V ratios of stations in the lake zone*

Figure 2 shows the $\hat{a}(f)$ of the H/V ratios (equation 2) with a 95% confidence interval (equation 3) at lake zone stations AP68, AU11, CE32 and MY19. Figure 2 also shows the TTF at the corresponding station and the first- fourth peaks of the TTF between which σ_i and r were computed and shown in the figure. H/V ratios of stations in the lakebed zone tend to have lower interevent variability than H/V ratios in the transition zone (Figure 3). In addition, the width of the peaks of the H/V ratio are thinner and there are multiple thin, distinct peaks. These peaks match up with the width and phase of the TTF computed at the corresponding station. The fundamental frequencies of these stations fall between 0.25 and 0.5 Hz, suggesting a greater depth to the deep deposits in the lakebed than the transition zone, an observation confirmed by depth to deep deposit maps (Moisés et al. 2016). The peaks could be an indicator of resonance, in which case the lake zone is well modeled by our one-layer simplification, or multiple significant impedance contrasts in the soil profile, such as the FHL. In future work, we plan on increasing the complexity of our soil model to include the FHL and LCF to see how they affect the TTF.

4.2 *H/V ratios in the transition zone*

Figure 3 shows the $\hat{a}(f)$ of the H/V ratios (equation 2) with a 95% confidence interval (equation 3) at transition zone stations DR16, GR27, ME52 and AU46. The peaks of $\hat{a}(f)$ of the transition zone stations in Figure 3 are wider than the peaks of $\hat{a}(f)$ of the lake zone stations
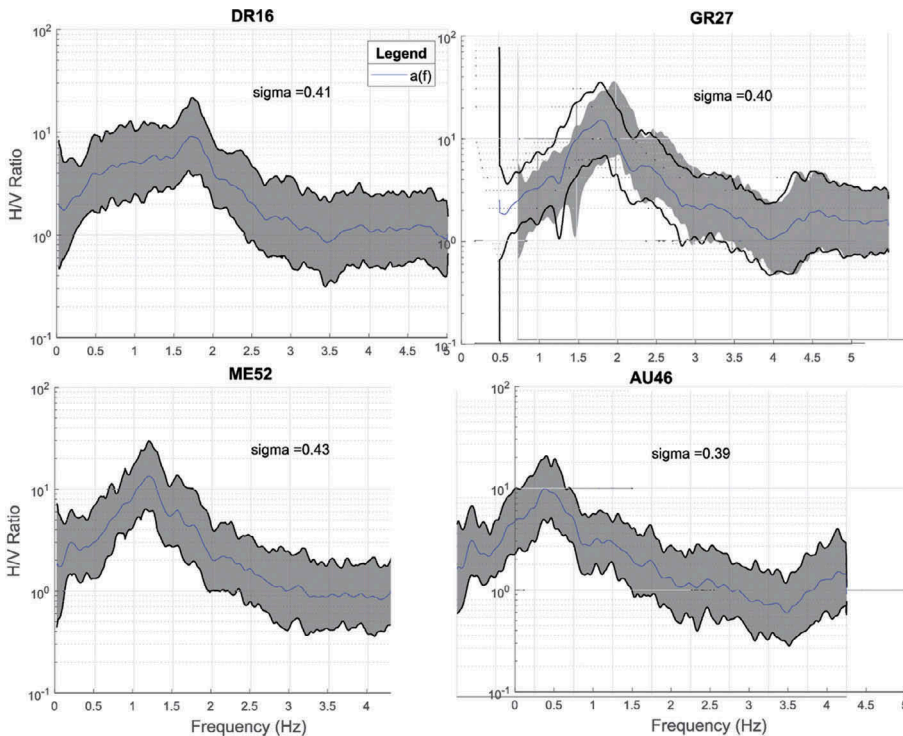

Figure 3. Selected H/V ratios from the transition zone, refer to Figure 1 to locate the stations. The blue line represents $\hat{a}(f)$ and the grey represents the confidence interval computed from equation 3. The σ_i values for stations DR16, GR27, ME52 and AU46 are 0.41, 0.40 and 0.43 and 0.39 respectively. Thus, they are all classified as high inter-event variability.

in Figure 2. This broadband peak likely indicates geologic conditions that do not conform to SH1D assumptions potentially due to wave scattering along the edge of the lakebed. This wide peak made fitting the TTF to the stations in the transition zone more challenging than fitting the TTF to the stations in the lake zone, suggesting that the lake zone is better modeled using SH1D assumptions. The interevent variability, σ_i, of the transition zone stations is greater than 0.35, classifying them as "high" interevent variability whereas σ_i of the lake zone stations in less than 0.35, classifying them as "low interevent variability.

The $\hat{a}(f)$ of the stations in the transition zone in Figure 3 have one significant peak at a frequency between 1-1.5 Hz. The frequency of the peak of $\hat{a}(f)$ of DR16 and GR27 is higher than the frequency of the peak of $\hat{a}(f)$ of ME52 and AU46, suggesting that DR16 and GR27 are located where it is shallower to the high velocity layer than at ME52 and AU46. DR16 and GR27 also have higher inter-event variability than ME52 and AU46, maybe due to more random scattering of wave energy in a more complex geological environment. The broadband peak is potentially due to a wider range of frequencies present as a function of the geology or an increase in damping or both. The fundamental frequencies of the examples provided are similar and represent an overall shape and trend in fundamental site frequency for stations in the transition zone.

We found that the amplitude of the TTF tended to be significantly lower than the $\hat{a}(f)$ ratio peaks. The amplitude is a function of the impedance contrast; thus, a higher deep deposit shear wave velocity will yield higher amplitudes in the TTF. We also constrained our inversion to a single soil layer over the deep deposit. In future work, we will allow for more variability in the soil profile and shear wave velocities to see if we can obtain a better fit to $\hat{a}(f)$.

The differential evolution algorithm worked well for finding TTFs in the lake zone because the lake zone has $\hat{a}(f)$ values that conform better to the SH1D assumptions. Despite the selection of the parameters for the high velocity layer our inversion for the TTF at stations in the transition zone didn't produce any TTFs with good fit to the corresponding $\hat{a}(f)$. The inversion failed to locate the peaks and could not match the width of the peak. The peaks of $\hat{a}(f)$ in the transition zone are wider than those in the lake and our bounding values of ${}^i Q_s^{-1}$ and depth missed the width of the transition zone $\hat{a}(f)$. Future work will address this issue.

5   CONCLUSIONS

Lermo and Chávez-Garcia (1993) found that when they compared Nakamura's H/V technique to standard spectral ratios with a reference site (Borcherdt, 1970), the H/V technique could provide a good first estimate of period and amplification (Lermo and Chávez-Garcia, 1993). In this study, we use the taxonomy from Thompson et al. (2012) adapted for Nakamura's H/V ratios to show that in the lake sediments of Mexico City, the H/V ratios have low inter-event variability and a good fit to the SH1D transfer function whereas in the transition zone, H/V ratios have higher inter-event variability, and lower goodness of fit to the SH1D transfer function, suggesting an increase in geological and site complexity. In this application, we don't have velocity profiles for each of the stations, so we estimate TTF by using a generic single layer profile for the region, where h is estimated from the ETF. This simple inversion breaks down for the transition zone where the ETF does not have simple SH1D resonant behavior. H/V ratios can therefore be used as a first estimate of site complexity in Mexico City by adapting the Thompson et al. (2012) taxonomy to H/V ratios.

REFERENCES

Boore, D. M. (2005) SMSIM-Fortran Programs for Simulating Ground Motion from Earthquakes: Version 2.3-A of OFR 96-80-A. United States Department of the Interior. U. S Geological Survey.

Butterworth, S., (1930) On the theory of filter amplifiers. Exp. Wirel. Wirel. Eng. 7, 536–541.

Campillo M., Gariel, J. C., Aki, K. Sanchez-Sesma, F.J. (1989). Destructive Strong Ground Motion in Mexico City: Source, Path, and Site Effects During Great 1985 Michoacan Earthquake Bulletin of the Seismological Society of America 79(6): 1718-1735.

Çelebi M, Sahakian V, Melgar D, Quintanar L. (2017) The 19 September 2017 M 7.1 Puebla-Morelos Earthquake: Spectral Ratios Confirm Mexico City Zoning. Bulletin of the Seismological Society of America. Vol. 20, No. 20.

Haskell N. A. (1953) The dispersion of surface waves on multilayered media. Bulletin of the Seismological Society of America; 72:17–34.

Haskell, N. A. (1960). Crustal Reflection of Plane SH Waves. Geophysical Research 65(12): 4147-4150.

Kaklamanos, J., Bradley, B.A., Thompson, E. M., Baise, L. G. (2013). Critical Parameters Affecting Bias and Variability in Site-Response Analyses Using Kik-net Downhole Array Data. Bulletin of the Seismological Society of America. Vol. 103, No. 3: 1733-1749.

Kaklamanos, J., Baise, L.G., Thompson, E.M., Dorfmann, L. (2015). Comparison of 1D linear, equivalent-linear, and nonlinear site response models at six KiK-net validation sites. Soil Dynamics and Earthquake Engineering 69, 207-219.

Kaklamanos, J., Bradley, B.A. (2018). Challenges in Predicting Seismic Site Response with 1D Analyses: Conclusions from 114 KiK-net Vertical Seismometer Arrays. Bulletin of the Seismological Society of America, Vol. 20, No. 20.

Lermo, J., and J. F. Chávez-García (1993). Site effect evaluation using spectral ratios with only one station, Bull. Seismol. Soc. Am. 83, 1574–1594.

Lermo J, Chávez-Garcia F.J. (1994) Site effect evaluation at Mexico City: dominant period and relative amplification from strong motion and microtremor records. Soil Dynamics and Earthquake Engineering. 13(1994): 413-423.

Lermo, J., and J. F. Chávez-García (1994). Are microtremors useful in site response evaluation? Bull. Seismol. Soc. Am. 84, no. 5, 1350–1364.

Moisés, J.C., Gabriel, A.G., Edgar, M.S. (2016) Geotechnical Zoning of Mexico Valley Subsoil. Ingeniería Investigación y Tecnología, volumen XVII (número 3), julio-septiembre 2016: 297-308.

Mooser, F., 1987. Antecedentes geológicos. In: Manual de Diseño Geotécnico, E. Tamez, E. Santoyo, F. Mooser and C. Gutiérrez, eds. (COVITUR, México, vol. 1).

Nakamura, Y. (1989) A Method for Dynamic Characteristics Estimation of Subsurface using Microtremor on the Ground Surface. Railway Technical Research Institute 30(1): 25-33.

Parolai, S., Bormann, P., Milkereit, C., (2002). New Relationships between Vs, Thickness of Sediments, and Resonance Frequency Calculated by the H/V Ratio of Seismic Noise for the Cologne Area (Germany). Bulletin of the Seismological Society of America, Vol. 92, No. 6, pp. 2521–2527, August 2002.

Rathje, E. M., Kottke, A. R., Trent, W. L. (2010). Influence of Input Motion and Site Property Variabilities on Seismic Site Response Analysis. Journal of Geotechnical and Geoenvironmental Engineering, 136(4).

Rodriguez-Marek, A., Montalva, G.A., Cotton, F., and Bonilla, F. (2011). Analysis of single-station standard deviation using the KiK-net data. Bull. Seism. Soc. Am. 101 (3), 1242-1258.

Romo, M.P., Jaime, A., Reséndiz, D (1988). The Mexico City Earthquake of September 19, 1985- General Soil Conditions and Clay properties in the Valley of Mexico. Earthquake Spectra, Vol 4, No. 4, 731-752.

Sanchez, R.J. (1989) Geology and tectonics of the basin of Mexico and their relationship with the damage caused by the earthquakes of September 1985. International Journal of Mining and Engineering, 1989, 7, 17-28.

Shearer PM, Orcutt JA. Surface and near-surface effects on seismic waves—theory and borehole seismometer results. Bulletin of the Seismological Society of America 1987;77(4):1168–1196.

Steidl JH, Tumarkin AG, Archuleta RJ. What is a reference site? Bulletin of the Seismological Society of America 1996;86(6):1733–1748.

Stephenson, B. Lomnitz, C. (2005). Shear-wave velocity profile at the Texcoco strong-motion array site, Valley of Mexico. Geofisca Internacional 44(1): 3-10.

Thomson WT. (1950). Transmission of elastic waves through a stratified solid. Journal of Applied Physics: 21:89–93.

Thompson EM, Baise LG, Tanaka K, Kayen RE. (2012) A taxonomy of site response complexity. Soil Dynamics and Earthquake Engineering. 41(2012): 32-43.

Thompson EM, Baise LG, Kayen RE, Guzina BB. (2009) Impediments to Predicting Site Response: Seismic Property Estimation and Modeling Simplifications. Bulletin of the Seismological Society of America. Vol. 99, No. 5: 2927-2949.

Yilar, E., Baise, L.G., Ebel, J.E. (2017) Using H/V measurements to determine depth to bedrock and Vs30 in Boston, Massachusetts. Engineering Geology 217, 12-22.

Zalachoris, G., and Rathje E.M. (2015). Evaluation of one-dimensional site response techniques using borehole arrays, J. Geotech. Geoenviron. Eng., 10.1061/(ASCE)GT.1943-5606.0001366, 04015053.